



An EQCM-D study of the influence of chloride on the lead anodic oxidation

Maiara O. Salles, Vitor L. Martins, Roberto M. Torresi, Mauro Bertotti*

Instituto de Química – Universidade de São Paulo, São Paulo, SP 05508-900, Brazil

ARTICLE INFO

Article history:

Received 21 March 2012
Received in revised form 4 June 2012
Accepted 5 June 2012
Available online 15 June 2012

Keywords:

Lead electrodeposition
Chloride effect
Quartz crystal microbalance
Stripping analysis
Scanning electron microscopy

ABSTRACT

The influence of chloride on the electrodeposition of lead films and their dissolution in anodic stripping voltammetric experiments was examined. Gold substrates were plated with lead films, and mass changes were monitored by using the electrochemical quartz crystal microbalance with dissipation factor (EQCM-D). The results showed that the amount of electrodeposited lead is slightly dependent on the chloride concentration. The charge/mass ratio data indicated the presence of Pb(I) and Pb(II) as a result of film dissolution, and the precipitation and deposition of PbCl_2 onto the electrode surface. Scanning electron microscopy images revealed that the morphology of the lead film was strongly influenced by chloride present in the plating solution and that much rougher films were obtained in comparison with those obtained in the absence of chloride. The rate of the anodic dissolution was higher for lead films with higher surface areas, which lead to an increase in their stripping voltammetric currents.

© 2012 Elsevier Ltd. All rights reserved.

1. Introduction

Electroanalytical methods for metal determination often require a preconcentration step in order to detect the analyte at very low concentrations. Mercury is the most commonly used electrode for such analyses in stripping voltammetry techniques [1–3], mainly due to the high hydrogen overvoltage and the ability of mercury to form amalgams with several metals. However, since mercury is a toxic metal, other materials such as bismuth and antimony have been used in stripping analyses [4–9]. The accumulation of the analyte can also be done directly at bare surfaces and the literature reports the use of carbon [10–12] and gold electrodes [13,14].

The electrochemical quartz crystal microbalance (EQCM) technique is widely used for measuring the change in the mass of an electrode while a film is deposited on or stripped off from the electrode surface. When an EQCM with dissipation (EQCM-D) is used, the recording of resonance frequencies of the electrode and the dissipation of a film during its electrodeposition or dissolution can provide certain information, e.g., about the mechanism by which the deposition or the dissolution occurs, deposition/dissolution efficiency (based on charge/mass ratio), and viscoelastic properties [15–18].

Several studies for analyzing the electrodeposition of lead onto different substrates by using the EQCM or EQCM-D have been performed by focusing, for instance, on the underpotential deposition

[17,19–21] and the effect of other substances, such as oxygen, sulfur, bismuth, and copper on the film deposition [16,22–24].

The determination of lead by stripping analysis using gold as a substrate has been reported in the literature [14,25–31]. In some reports, the influence of chloride on the lead electrodeposition has been described, [14,31,32] but to the best of our knowledge, this influence has not been extensively investigated and characterized. The use of EQCM-D and scanning electron microscopy (SEM) facilitated a better understanding of this phenomenon by showing clearly the influence of chloride anions on the deposition and dissolution processes. This understanding is very important in evaluating the influence of sample composition on the electroanalytical determination of Pb(II) and in ensuring reliable analysis.

2. Experimental

2.1. Reagents

All reagents were of analytical grade and used without any further purification. $\text{Pb}(\text{NO}_3)_2$, KCl, and $\text{K}_3[\text{Fe}(\text{CN})_6]$ solutions were prepared by dissolving the reagents in deionized water processed through a water purification system ($18.0 \text{ M } \Omega \text{ cm}^{-1}$, Nanopure Infinity, Barnstead, Iowa, USA). The nitric acid solution was prepared by diluting the stock solution, as necessary. All reagents were obtained from Merck (Darmstadt, Germany).

2.2. Square wave voltammetry experiments

An Autolab PGSTAT 30 (Eco Chemie) was used for experiments with square wave voltammetry (SWV), a technique that has been

* Corresponding author. Tel.: +55 11 30912694.

E-mail address: mbertott@iq.usp.br (M. Bertotti).

largely used to improve the sensitivity of analytical determinations [33]. A gold disc microelectrode was used as the working electrode for the stripping analysis. A homemade Ag/AgCl_(sat. KCl) electrode, inserted in a separate compartment to avoid chloride contamination, and a platinum wire were used as reference and counter electrodes, respectively. Before each experiment, a positive potential ($E_{\text{cleaning}} = 0.70\text{ V}$) was applied to the electrode for 2 min ($t_{\text{cleaning}} = 120\text{ s}$). Lead was then deposited at the microelectrode surface ($E_{\text{deposition}} = -0.70\text{ V}$) in solutions containing 0.1% (m/v) HNO₃, 0.1 $\mu\text{mol L}^{-1}$ Pb²⁺ with different chloride concentrations (in the range 0–50 mmol L⁻¹). Lead was stripped off by SWV at the same solution employed in the deposition step. The potential was scanned from -0.70 to 0.10 V and the potential step (E_{step}), potential amplitude ($E_{\text{amplitude}}$) and frequency parameters were 5 mV, 25 mV and 300 Hz, respectively.

The gold microelectrode was fabricated as follows: a gold fiber (diameter = 25 μm , Goodfellow Cambridge Ltd., Cambridge, England) was connected to a Ni/Cr wire with silver ink conductive paint (Joint Metal Comércio Ltda, São Paulo, Brazil), and then inserted into a glass capillary and flame-fuse sealed in the tip of the glass capillary. The radius of the working microelectrode was determined by measuring the steady-state current in a K₃[Fe(CN)₆] solution of known concentration, and the value was found to be 12.5 μm .

2.3. Scanning electron microscopy experiments

A scanning electron microscope (FESEM JSM-7401F, JEOL) using a LEI detector, 1.0 kV accelerating voltage and 8 mm working distance was used for image acquisition of different lead films electrodeposited onto gold microfibers ($r = 63\ \mu\text{m}$). Electrodeposition for 480 s was accomplished at -0.70 V using solutions containing 0.1% (m/v) HNO₃ and 0.1 $\mu\text{mol L}^{-1}$ Pb²⁺, with different chloride concentrations (in the range 0–75 mmol L⁻¹).

2.4. Electrochemical quartz crystal microbalance with dissipation experiments

The EQCM-D measurements were carried out with a QCM-D system from Q-Sense (Göteborg, Sweden) and an Autolab PGSTAT 30 (Eco Chemie, The Netherlands), by simultaneously monitoring the changes in resonance frequency (Δf), dissipation (ΔD) and current. The change in Δf can be related to the change in mass (Δm) in the case of a rigid film by using the Sauerbrey equation (1) [34]:

$$-\Delta f_n = \left(\frac{C}{n}\right) \Delta m \quad (1)$$

where the mass sensitivity C was 17.7 ng cm⁻² Hz⁻¹ and n is the overtone (1, 3, 5, 7, 9, 11, and 13). A gold electrode (Q-Sense) was used as the working electrode after cleaning it with an alkaline piranha solution (1:1:5 H₂O₂/NH₄OH/H₂O mixture at 70 °C) for 5 min. The electrode was then rinsed with deionized water, sonicated for 5 min in deionized water and ethanol, dried with a nitrogen stream, and then kept in a UV/Ozone cleaner (ProCleaner Plus BioForce) for 15 min prior to use. A Pt spiral wire and a homemade Ag/AgCl_(sat. KCl), which was inserted in another compartment to avoid chloride contamination, were employed as counter and reference electrodes, respectively.

The studies regarding the film deposition (at -0.70 V) were performed in solutions containing 0.1% (m/v) HNO₃ and 5 mmol L⁻¹ Pb²⁺ with different chloride concentrations (in the range 0–75 mmol L⁻¹). In order to examine the film dissolution, the electrodeposition was carried out at potentiostatic conditions (-0.70 V) in solutions containing 0.1% (m/v) HNO₃, 5 mmol L⁻¹ Pb²⁺ and different chloride concentrations (in the range 0–75 mmol L⁻¹). Then, the film was stripped off using linear sweep voltammetry (LSV) from -0.70 to 0.70 V at different scan rates (from 1 to

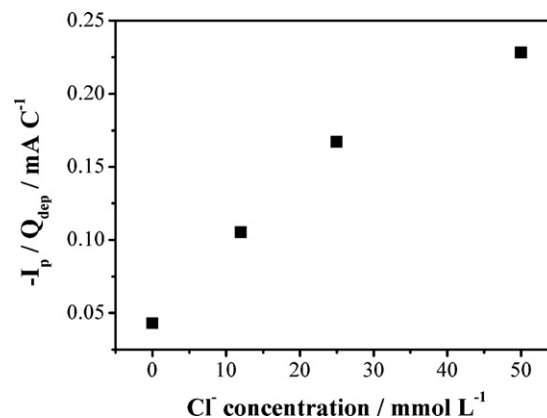


Fig. 1. Stripping peak current/charge deposition as a function of Cl⁻ concentration. Lead analysis performed using square wave voltammetry on a gold microelectrode ($r = 12.5\ \mu\text{m}$) with solutions containing 0.1% (m/v) HNO₃, 0.1 $\mu\text{mol L}^{-1}$ Pb²⁺ and varying Cl⁻ concentrations (12.5, 25 and 50 mmol L⁻¹) in a quiescent solution. Parameters used: $E_{\text{cleaning}} = 0.70\text{ V}$, $t_{\text{cleaning}} = 120\text{ s}$, $E_{\text{deposition}} = -0.70\text{ V}$, $t_{\text{deposition}} = 480\text{ s}$, $E_{\text{final}} = 0.10\text{ V}$, Frequency: 300 Hz, $E_{\text{step}} = 5\text{ mV}$, $E_{\text{amplitude}} = 25\text{ mV}$, $t_{\text{equilibrium}} = 10\text{ s}$.

100 mV s⁻¹). Experiments involving film dissolution were performed using solutions containing 0.1% (m/v) HNO₃ and different concentrations of chloride and Pb²⁺. As in the deposition step, chloride concentrations were in the range of 0–75 mmol L⁻¹. Pb²⁺ was mainly at a concentration equal to 5 mmol L⁻¹ unless in one of the experiments, where a free lead solution was used. At this experiment, a peristaltic pump (Gilson MINIPULS Evolution, France) was used to slowly exchange the deposition solution from the dissolution solution.

3. Results and discussion

3.1. Square wave voltammetry experiments

Preliminary experiments were carried out to confirm the influence of chloride on the lead stripping voltammetric oxidation peak. Data were obtained by square wave voltammetry, as described in the experimental section, using a gold microelectrode in solutions containing 0.1% (m/v) HNO₃ and 0.1 $\mu\text{mol L}^{-1}$ Pb²⁺ in the presence of different chloride concentrations (range of 0–50 mmol L⁻¹). Fig. 1 shows the ratio of the peak current ($E_{\text{peak}} = 0.10\text{ V}$) recorded during the stripping step to the charge associated with the lead electrodeposition process, under each experimental condition. Since the SWV current was normalized by the charge (typical values ranged between -20 and -30 μC), the increase in this ratio as a function of the chloride concentration confirms the significant influence of the halide on the stripping response, as already reported in the literature [14,31,32].

3.2. Effect of chloride on film deposition

The influence of chloride on the electrodeposited lead film was firstly studied by scanning electronic microscopy (SEM). Images of the gold surface were taken after lead electrodeposition performed in the absence and presence of 25, 50, and 75 mmol L⁻¹ chloride under potentiostatic conditions ($E = -0.70\text{ V}$). In the absence of chloride, a flat surface was obtained (Fig. 2(A)), whereas much rougher surfaces were seen when the lead was plated in solutions containing chloride (Fig. 2(B–D)). These results clearly demonstrate the influence of chloride on the morphology of the electrodeposited lead film. Jones et al. reported that differences in stripping voltammetry can be explained by the differences in the orientation and morphology of the deposited film, since the surface structure can affect the stripping process [35].

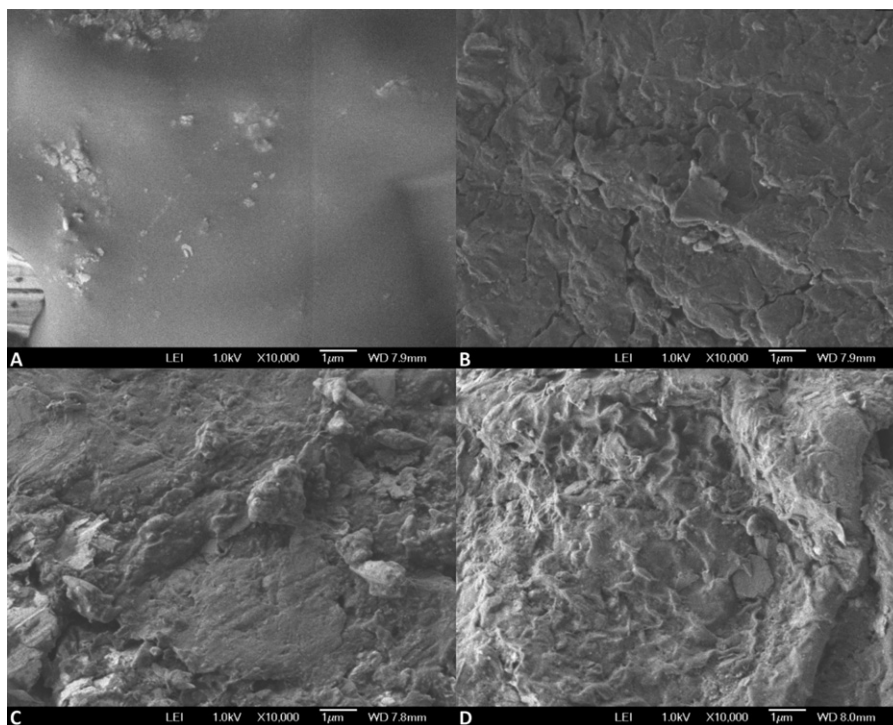


Fig. 2. Scanning electron micrograph of a lead film electrodeposited on a gold fiber ($r = 63 \mu\text{m}$) under potentiostatic conditions ($E_{\text{dep}} = -0.70 \text{ V}$, $t_{\text{dep}} = 480 \text{ s}$) using a solution containing $0.1\% \text{ (m/v) HNO}_3$ and $5 \text{ mmol L}^{-1} \text{ Pb}^{2+}$ in the absence (A) and presence of 25 (B), 50 (C), and 75 (D) $\text{mmol L}^{-1} \text{ Cl}^-$.

In addition to the effect on the film morphology, chloride could also have an influence on the amount of electrodeposited lead. In order to examine this question, lead film formation on the gold electrode (crystal quartz) was examined by EQCM-D in the absence and presence of chloride at various concentrations (25, 50, and 75 mmol L^{-1}). During the experiments, the changes in frequency (Δf) and film dissipation (ΔD) were recorded for all overtones ($n = 1, 3, 5, 7, 9, 11, \text{ and } 13$). Fig. 3(Ia) shows a typical profile of Δf and ΔD vs. time obtained during the lead film deposition and subsequent dissolution in the absence of chloride. Fig. 3(Ib) shows the applied potential/time program used to obtain the aforementioned EQCM-D experiment. At the beginning of the experiment (t_1), no potential was applied to the electrode and it remained at open circuit. The decrease in Δf at t_2 is a consequence of the increase in the mass due to the beginning of lead electrodeposition ($E = -0.70 \text{ V}$). At t_3 , a potential sweep was imposed on the working electrode from -0.70 V to 0.70 V at 10 mV s^{-1} . The starting potential was selected as -0.70 V to avoid the chemical dissolution of the lead film due to dissolved oxygen. Lead continued to be electrodeposited up to -0.40 V . At this potential (t_4), Δf started to increase, indicating the beginning of metallic lead dissolution. Δf values approached 0 Hz at t_5 , indicating that lead stripping was complete. Δf and ΔD continued to be measured at open circuit for approximately 1 min. Neither the frequency nor the dissipation varied significantly among the overtones; hence, the formed film can be considered to be acoustically rigid. In addition, the change in the film dissipation is almost insignificant when compared to the frequency variation, confirming the rigid nature of the lead film formed on the electrode surface. In the case of an acoustically rigid film, the Sauerbrey equation can be used to obtain information on the mass change from the frequency change (Eq. (1)). A similar Δf and ΔD profile was observed when the deposition was performed with solutions containing chloride (from 25 to 75 mmol L^{-1}), therefore those films have also a rigid nature and the Sauerbrey equation can be applied to the results obtained at these experimental conditions.

The current dependence on time during electrodeposition in all the experiments described above (Pb^{2+} deposited onto a crystal quartz gold electrode in solutions containing different chloride concentrations (0, 25, 50 and 75 mmol L^{-1}) at -0.70 V) and the mass change values (determined from the frequency changes for the 5th overtone, chosen arbitrarily) were investigated. A plot of charge as a function of the mass change in the deposition process (Fig. 3(II)) was obtained by calculating the charge by integrating the current/time profile. A linear relationship between charge and mass was found for all supporting electrolyte solutions used in the experiments. Since the slope values (charge/mass) of the straight lines presented no significant variation, chloride does not play an important role in the charge/mass ratio during the electrodeposition process.

The mean slope value was $(815 \pm 55) \text{ C g}^{-1}$, which is lower than expected when taking into account the electroreduction from Pb^{2+} to Pb (931.3 C g^{-1}). However, this can be explained by considering the possible confinement of water molecules into inhomogeneities in the surface, as proposed by Schumacher et al. [36]. As shown by the SEM images, the presence of chloride in the deposition solution results in films with different roughness and the presence of water inside the inhomogeneities of the films can increase the measured mass value without decreasing proportionally the charge, resulting in a decrease of the charge/mass ratio.

3.3. Effect of chloride on film dissolution

Lead is oxidized during the voltammetric stripping step, and the influence of chloride on the rate of this process was investigated. To this end, the mass change was recorded during the dissolution process at different scan rates in a preliminary experiment carried out in the absence of chloride. The amount of lead deposited on the electrode surface in the absence of chloride was maintained constant in all experiments by controlling the charge deposition (-23 mC). Fig. 4 shows that the mass returns to its initial value and that this is independent of the scan rate, which was varied

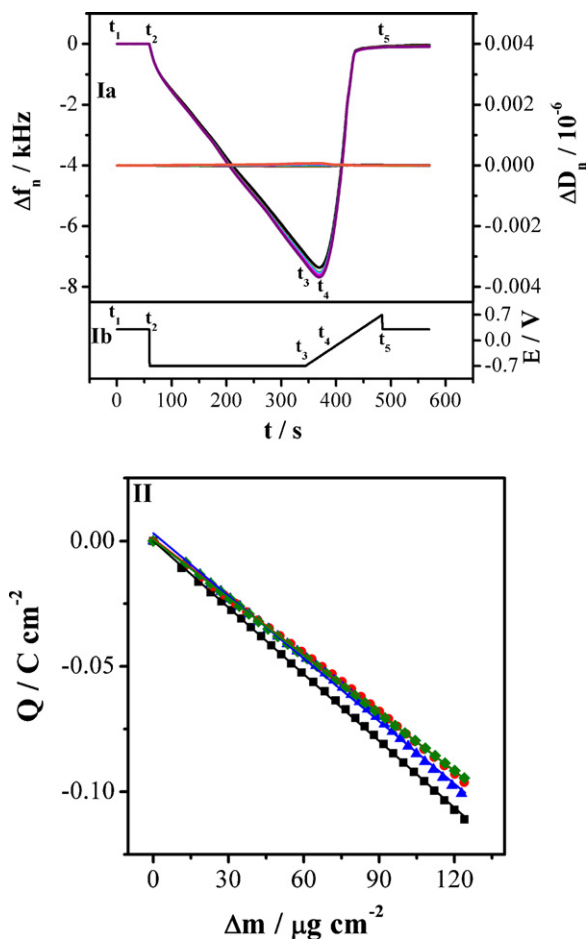


Fig. 3. (Ia) Dependence of frequency (Δf_n) and dissipation (ΔD_n) at different overtones ($n = 1, 3, 5, 7, 9, 11$ and 13) as functions of time for lead films electrodeposited in a resonant crystal quartz in a 0.1% (m/v) HNO_3 , 5 mmol L^{-1} Pb^{2+} solution in absence of Cl^- according to the potential program showed in Fig. 3 (Ib): indicated by: (t_1) open circuit (0.40 V); (t_2) -0.70 V ; (t_3) beginning of the potential sweep at 10 mV s^{-1} ; (t_4) initial of lead film dissolution (-0.40 V); (t_5) end of the potential sweep (0.70 V). (II) Relationship between deposition charge and mass deposited in solutions with 0 (■), 25 (●), 50 (▲), and 75 (◆) mmol L^{-1} Cl^- . Lead films were electrodeposited in the same conditions as Fig. 3(Ia).

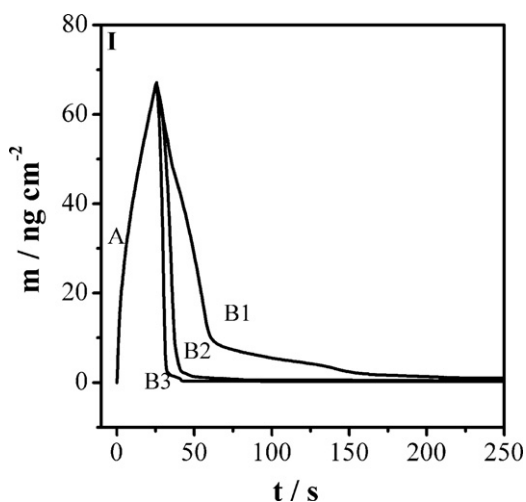


Fig. 4. Mass change as a function of time after lead film electrodeposited under potentiostatic conditions ($E_{\text{dep}} = -0.70 \text{ V}$) from a solution containing 0.1% (m/v) HNO_3 and 5 mmol L^{-1} Pb^{2+} in a resonant crystal quartz. The value of Q_{dep} is -23 mC (A) and film dissolution was performed at 1 (B1), 20 (B2) and 100 (B3) mV s^{-1} .

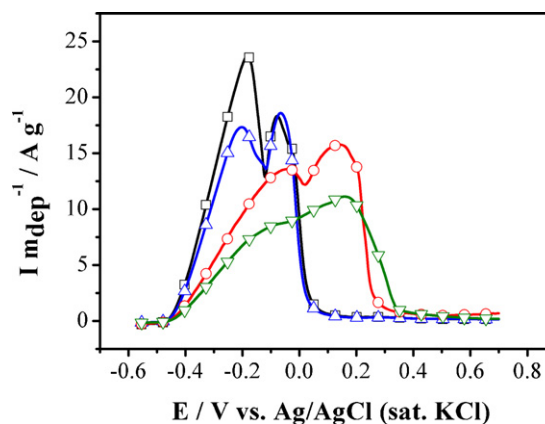


Fig. 5. Linear sweep voltammograms recorded at 10 mV s^{-1} in the presence (□ and ▲) and absence (○ and ▼) of 50 mmol L^{-1} chloride after lead deposition performed in a resonant crystal quartz under potentiostatic conditions ($E_{\text{dep}} = -0.70 \text{ V}$) in the presence (□ and ○) and absence (▲ and ▼) of 50 mmol L^{-1} chloride with mass cut off ca. $124 \mu\text{g cm}^{-2}$. Note: current and charge were normalized by total deposited mass (m_{dep}) after the complete exchange of deposition solution (0.1% (m/v) HNO_3 and 5 mmol L^{-1} Pb^{2+} (▲ and ▼) or 0.1% (m/v) HNO_3 , 5 mmol L^{-1} Pb^{2+} and 50 mmol L^{-1} chloride (□ and ▲)) by dissolution solution (0.1% (m/v) HNO_3 (○ and ▼) or 0.1% (m/v) HNO_3 and 50 mmol L^{-1} chloride (□ and ▲)).

from 1 to 100 mV s^{-1} . Further, one can confirm that during this time window the film was completely stripped off and there was no kinetic problem associated with the film dissolution.

Subsequently, in order to evaluate the influence of chloride on anodic lead dissolution, four lead deposits were prepared: two in the absence (▲ and ▼) and two in the presence of chloride (□ and ○); the films were then stripped off in the absence (○ and ▼) and presence of chloride (□ and ▲). The deposition was performed under potentiostatic conditions (-0.70 V), and when the amount of mass deposited reached ca. $24 \mu\text{g cm}^{-2}$, the electrolyte was replaced with a new Pb^{2+} -free one, while maintaining the potential at -0.70 V . During the solution exchange, no mass variation was observed and the cathodic current decreased to values less than $1 \mu\text{A cm}^{-2}$. Then, linear sweep voltammograms (LSV) experiments were carried out at -0.70 V to 0.70 V in the absence and presence of chloride (50 mmol L^{-1}). Fig. 5 shows the voltammograms obtained (current was normalized by total deposited mass, m_{dep}) after dissolution of each deposit. From the obtained results, two main conclusions can be drawn. At the same conditions of deposition (absence of chloride, (▲ and ▼) and presence of chloride (□ and ○)), the film oxidation takes place at less positive potential values when chloride is present in the solution during the dissolution step (curves marked with black square (□) and up blue triangle (▲)), as a consequence of the formation of stable complexes with chloride, i.e., PbCl^+ (stability constant = $10^{1.59}$) [37]. Moreover, the peak current in the presence of chloride (curves marked with black square (□) and up blue triangle (▲)) was much higher when compared to the one in the chloride-free electrolyte (curves marked with red circle (○) and down green triangle (▼)). This indicates that the halide plays an important role in the stripping off of the lead film, regardless of whether the deposition was performed in the presence or absence of chloride. In addition, considering the same dissolution solution (presence of chloride – curves marked with black square (□) and up blue triangle (▲) and absence of chloride – curves marked with red circle (○) and down green triangle (▼)), higher peak current values were always observed when the deposition was performed in the presence of chloride (□ and ○), as a result of the increase in the surface roughness.

The correlation between the anodic current during the dissolution of the lead film and dm/dt (i.e., the derivative of mass m with respect to time t) was also examined. This was accomplished

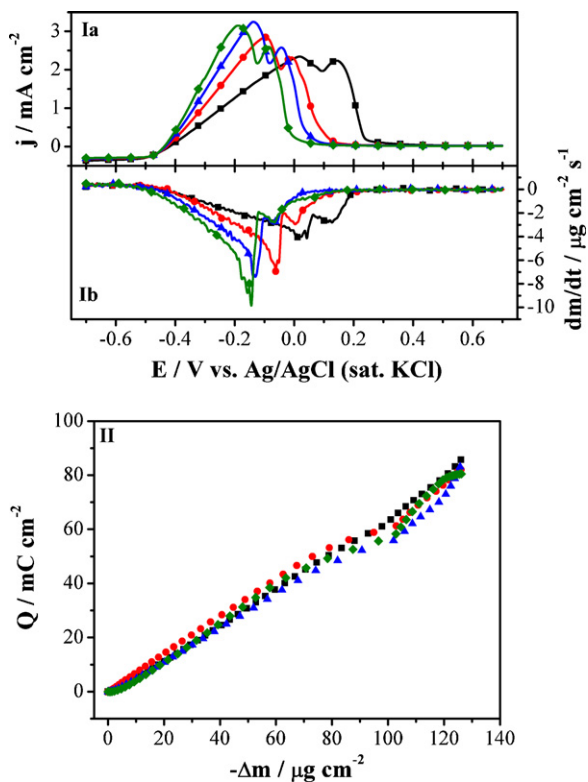


Fig. 6. (Ia) Linear sweep voltammograms (LSVs) recorded at 10 mV s^{-1} in solutions containing $0.1\% (\text{m/v}) \text{ HNO}_3$ and $5 \text{ mmol L}^{-1} \text{ Pb}^{2+}$ and having chloride concentrations of 0 (■), 25 (●), 50 (▲), or 75 (◆) mmol L^{-1} . Lead film deposition was performed in a resonant crystal quartz under potentiostatic conditions ($E_{\text{dep}} = -0.70 \text{ V}$) with a mass cut off of $133 \mu\text{g cm}^{-2}$ using the same solution that was used to obtain the LSVs. (Ib) Derivative of mass as a function of potential, which was calculated from the LSV. (II) Relationship between dissolution charge and mass loss in the presence of 0 (■), 25 (●), 50 (▲), or 75 (◆) $\text{mmol L}^{-1} \text{ Cl}^-$.

by electrodeposition of lead films and subsequent linear sweep voltammetry (LSV) performed in the same solution. Four solutions were used in this experiment, each of them containing different chloride concentrations (0 , 25 , 50 , and 75 mmol L^{-1}). The deposition was carried out under potentiostatic conditions (-0.70 V) with controlled mass deposition (*ca.* $124 \mu\text{g cm}^{-2}$) and the LSV was performed from -0.70 V to 0.70 V at 10 mV s^{-1} . During the LSV, an increase in the mass due to the deposition of the lead film was observed until the potential reached -0.40 V , and this resulted in a total deposited mass of *ca.* $133 \mu\text{g cm}^{-2}$. Fig. 6(Ia) shows that the anodic oxidation peaks changed with increasing chloride concentration, despite the fact that the amount of electrodeposited lead was always the same (*ca.* $133 \mu\text{g cm}^{-2}$). In all cases, two anodic peaks were noticed and these shifted to less positive potentials as the concentration of chloride increased, as was observed in Fig. 5. To confirm that both anodic peaks are associated with the oxidation of lead, dm/dt values were calculated. Since $m = q(M/nF)$ (where q is the charge, M is the molar mass, n is the number of electrons involved in the reaction, and F is the Faraday constant), the derivative of mass with respect to time is proportional to the current. The profile of the dm/dt vs. E plots is similar to those of the voltammograms, as seen in Fig. 6(Ib), so it can be concluded that both anodic processes are related to the lead stripping. By analyzing changes in dm/dt values, especially in the potential region from -0.70 to -0.20 V , an interesting observation is made: the dissolution rate increases with the increase in the chloride concentration.

From this same set of experiments, it is also possible to analyze the relationship between the anodic charge (obtained by integrating the current/time profile shown in Fig. 6(Ia)) and mass loss; this relationship is shown in Fig. 6(II). Since the total deposited mass

was $133 \mu\text{g cm}^{-2}$, the charge expected for the dissolution process should be 123.9 mC cm^{-2} , assuming a two-electron process. However, in all cases, the total charge value obtained experimentally was approximately 28% lower than expected. Gioda et al. have proposed the formation of adsorbed Pb^+ in HClO_4 solutions and El Aal et al. have also proposed the presence of the same ad-ion in HCl medium [38,39]. Hence, the lower charge value obtained could be attributed to the partial formation of Pb^+ during the anodic dissolution of the film.

In addition, from Fig. 6(II), two linear regions with different slopes are obtained in all the experiments, in the absence or presence of chloride. The first region (until approximately $100 \mu\text{g cm}^{-2}$) is related to the first voltammetric peak observed in Fig. 6(Ia), and the charge/mass ratio values were found to be 646.2 , 705.6 , 615.6 , and 708.7 C g^{-1} for experiments performed in solutions containing 0 , 25 , 50 , and $75 \text{ mmol L}^{-1} \text{ Cl}^-$, respectively. The theoretical charge/mass ratio for the Pb/Pb^{2+} couple is 931.3 C g^{-1} , and for the Pb/Pb^+ couple this value is 465.6 C g^{-1} . However, all charge/mass ratio values experimentally obtained were found to be between these limits. Hence, at this first region, which corresponds to the first oxidation peak, both reactions (Pb/Pb^+ and Pb/Pb^{2+}) are likely to occur, independent of the concentration of chloride. The second region is related to the second voltammetric peak and the charge/mass ratio values were 845.6 , 874.5 , 997.0 , and 1117 C g^{-1} for solutions with different chloride concentrations (0 , 25 , 50 , and 75 mmol L^{-1} respectively). Charge/mass values that were higher than that expected for a two-electron process were obtained in solutions containing greater chloride concentrations (50 – 75 mmol L^{-1}). A possible explanation involves the deposition of PbCl_2 onto the electrode surface [39–41], as the concentration of $\text{Pb}(\text{II})$ at the electrode surface is higher at more positive potentials. Thus, the mass decrease due to lead oxidation is partially compensated by the deposition of PbCl_2 , resulting in the observed increase in the charge/mass ratio.

4. Conclusions

Lead stripping current increases with increasing chloride concentration of the electrodeposition solution, and this effect was examined by employing voltammetry, SEM and EQCM-D. The presence of chloride in the electrodeposition solution contributes to the increase in roughness of the lead film, which was confirmed by SEM images. As a consequence, stripping current peaks change significantly for films that are prepared with the same amount of lead but that have different morphologies, as shown by the electrochemical crystal microbalance experiments. EQCM-D experimental results showed that the amount of lead deposited on the gold electrode depends slightly on the concentration of chloride. Similarly, the electrodeposition efficiency (charge/mass ratio) is the same for all tested chloride concentrations; however, the value obtained is smaller than the theoretically calculated one, indicating that water may be trapped in the pores of these rough lead films. The analysis of current, mass changes, and charge dissolution during linear sweep voltammetry experiments in the absence and presence of chloride confirmed the influence of the halide on the dissolution process. The increase in the halide concentration of the supporting electrolyte solution results in a pronounced potential shift towards less positive values, as a consequence of the thermodynamically favored formation of complex species of lead ions and chloride. Peak current values were much higher in the presence of chloride, charge/mass ratio values indicate the presence of $\text{Pb}(\text{I})$, in addition to $\text{Pb}(\text{II})$, during the anodic dissolution and the rate of lead dissolution is enhanced in the case of films with increased surface area.

The results shown in this work confirm that plating lead films under differing experimental conditions, especially in the presence

of halides, results in the formation of films with different roughness, and this, in turn, can result in significantly different stripping currents. In such conditions (e.g., lead determination in seawater), the use of the standard addition method is strongly recommended, since the added spikes behave in a manner identical to that of the sample analyte, thereby compensating for the influence of chloride.

Acknowledgments

The authors acknowledge CNPq and FAPESP (09/53199-3) for financial support. MOS and VLM thank FAPESP (06/60078-0 and 09/09209-4) for the fellowships.

References

- [1] K.Z. Brainina, N.A. Malakhova, N.Y. Stojko, *Fresenius Journal of Analytical Chemistry* 368 (2000) 307.
- [2] A. Economou, P.R. Fielden, *Analyst* 128 (2003) 205.
- [3] O. Mikkelsen, K.H. Schroder, *Electroanalysis* 15 (2003) 679.
- [4] A. Economou, *TrAC, Trends in Analytical Chemistry* 24 (2005) 334.
- [5] J. Wang, *Electroanalysis* 17 (2005) 1341.
- [6] I. Svancara, K. Vytras, *Chemické Listy* 100 (2006) 90.
- [7] I. Svancara, C. Prior, S.B. Hocevar, J. Wang, *Electroanalysis* 22 (2010) 1405.
- [8] M.O. Salles, A.P.R. de Souza, J. Naozuka, P.V. de Oliveira, M. Bertotti, *Electroanalysis* 21 (2009) 1439.
- [9] M. Slavec, S.B. Hocevar, L. Baldrianova, E. Tesarova, I. Svancara, B. Ogorevc, K. Vytras, *Electroanalysis* 22 (2010) 1617.
- [10] I. Svancara, K. Vytras, J. Barek, J. Zima, *Critical Reviews in Analytical Chemistry* 31 (2001) 311.
- [11] K.C. Honeychurch, J.P. Hart, *TrAC, Trends in Analytical Chemistry* 22 (2003) 456.
- [12] K. Kalcher, I. Svancara, M. Buzuk, K. Vytras, A. Walcarius, *Monatshfte für Chemie* 140 (2009) 861.
- [13] A.P.R. de Souza, A.S. Lima, M.O. Salles, A.N. Nascimento, M. Bertotti, *Talanta* 83 (2010) 167.
- [14] E.M. Richter, J.J. Pedrotti, L. Angnes, *Electroanalysis* 15 (2003) 1871.
- [15] D.M. Soares, S. Wasle, K.G. Weil, K. Doblhofer, *Journal of Electroanalytical Chemistry* 532 (2002) 353.
- [16] K. Wagner, J.W. Strojek, K. Koziel, *Analytica Chimica Acta* 455 (2002) 69.
- [17] O. Melroy, K. Kanazawa, J.G. Gordon, D. Buttry, *Langmuir* 2 (1986) 697.
- [18] M.R. Deakin, O. Melroy, *Journal of Electroanalytical Chemistry* 239 (1988) 321.
- [19] Y. Lim, E. Hwang, *Bulletin of the Korean Chemical Society* 17 (1996) 1091.
- [20] X.Q. Zeng, S. Bruckenstein, *Journal of the Electrochemical Society* 146 (1999) 2555.
- [21] M.J. Henderson, E. Bitziou, A.R. Hillman, E. Vieil, *Journal of the Electrochemical Society* 148 (2001) E105.
- [22] D. Pech, T. Brousse, D. Belanger, D. Guay, *Electrochimica Acta* 54 (2009) 7382.
- [23] J.S. Gordon, V.G. Young, D.C. Johnson, *Journal of the Electrochemical Society* 141 (1994) 652.
- [24] H. Saloniemi, M. Kemell, M. Ritala, M. Leskela, *Thin Solid Films* 386 (2001) 32.
- [25] M.F.M. Noh, I.E. Tothill, *Analytical and Bioanalytical Chemistry* 386 (2006) 2095.
- [26] P. Masawat, S. Liawruangrath, *Chiang Mai Journal of Science* 35 (2008) 355.
- [27] S. Laschi, I. Palchetti, M. Mascini, *Sensors and Actuators B: Chemical* 114 (2006) 460.
- [28] C. Garnier, L. Lesven, G. Billon, A. Magnier, O. Mikkelsen, I. Pizeta, *Analytical and Bioanalytical Chemistry* 386 (2006) 313.
- [29] Y. Bonfil, M. Brand, E. Kirova-Eisner, *Analytica Chimica Acta* 464 (2002) 99.
- [30] H. Shen, J.E. Mark, C.J. Seliskar, H.B. Mark, W.R. Heineman, *Journal of Solid State Electrochemistry* 1 (1997) 241.
- [31] A. Mandil, L. Idrissi, A. Amine, *Microchimica Acta* 170 (2010) 299.
- [32] M.O. Salles, J. Naozuka, M. Bertotti, *Microchemical Journal* 101 (2012) 49.
- [33] J.G. Osteryoung, R.A. Osteryoung, *Analytical Chemistry* 57 (1985) A101.
- [34] G. Sauerbrey, *Zeitschrift Für Physik* 155 (1959) 206.
- [35] S.E.W. Jones, K.E. Toghill, S.H. Zheng, S. Morin, R.G. Compton, *Journal of Physical Chemistry C* 113 (2009) 2846.
- [36] R. Schumacher, G. Borges, K.K. Kanazawa, *Surface Science* 163 (1985) L621.
- [37] S. Kotrly, L. Sucha, *Handbook of Chemical Equilibria in Analytical Chemistry*, Ellis Horwood Limited, New York, 1985.
- [38] A.S. Gioda, M.C. Giordano, V.A. Macagno, *Journal of the Electrochemical Society* 124 (1977) 1324.
- [39] E.E.A. El Aal, S.A. El Wanees, *Corrosion Science* 51 (2009) 458.
- [40] R.G. Barradas, K. Belinko, J. Ambrose, *Canadian Journal of Chemistry-Revue Canadienne De Chimie* 53 (1975) 389.
- [41] S.S.A. Elrehim, A.M.A. Elhalim, E.E. Foad, *Surface Technology* 18 (1983) 313.